

## Tunneling Potential Barrier Dependence of Electron Spin Polarization

S. F. Alvarado

*IBM Research Division, Zurich Research Laboratory, 8803 Rüschlikon, Switzerland*

(Received 8 March 1995)

Scanning tunneling microscopy experiments reveal that the degree of spin polarization of electrons tunneling from Ni into a semiconductor increases with decreasing potential barrier thickness. The results show that the highly polarized  $3d$  bands as well as the low-polarized  $4sp$  bands contribute to the tunneling current and that the ratio of their tunneling probabilities depends on the potential barrier thickness and height. Furthermore, the tunneling potential barrier for the  $3d$ -like levels is estimated to be  $\sim 1$  eV higher than for the  $4sp$  contribution.

PACS numbers: 73.40.Gk, 72.15.Gd, 75.50.Rr, 78.60.Fi

The study of the injection process of spin-polarized electrons from a ferromagnetic material into a nonmagnetic material is of importance for the understanding of the physics of giant magnetoresistance and of the polarized electron transport in multilayer and granular systems, in which the magnetic coupling is mediated by a nonmagnetic material. Layered and granular exchange-coupled devices are currently the subject of intensive theoretical and experimental research because of their repercussions in information storage technology [1–3]. The efficiency of injecting spin-polarized charge carriers from material  $A$  to material  $B$  depends on the details of the electronic potential at the interface between the materials. This Letter presents scanning tunneling microscopy (STM) results that characterize some features of the potential barrier that influence the injection of spin-polarized electrons from a ferromagnetic metal into a semiconductor. Essentially, the experiment consists of measuring the spin polarization of electrons tunneling at constant energy as a function of the width of the tunneling potential barrier. The barrier width is varied by changing the tunneling current while keeping a fixed tunneling voltage. According to theoretical models [4–7], the tunneling current emitted from the ferromagnetic metal originates from the highly polarized and localized  $3d$ -like states and from the low polarized, delocalized,  $4sp$ -like states. Ideally, maximum spin polarization is expected when only the  $3d$ -like levels contribute to the current injected across the tunneling barrier potential. It is expected, however, that the  $sp$ -like states, given their highly delocalized nature, contribute substantially to the tunneling current, despite the fact their density of states is 1 order of magnitude smaller than that of the  $3d$  levels. On the other hand, it has also been noted [8] that it is necessary to distinguish between delocalized  $d_i$  and localized  $d_l$ -like electrons of  $E_g$  symmetry at  $\Gamma$ . Actually, dominant  $d_l$ -like tunneling has been proposed [8] as a simple explanation for the spin polarization measured on metal-oxide-superconductor junctions [9] at liquid-He temperatures for energies of a few meV. For tunneling through a vacuum barrier at the experimental conditions discussed here, however, an interpretation of the data in

terms of dominant  $d_l$ -like tunneling does not seem to be applicable (see below). The spin polarization of electrons tunneling from  $3d$  ferromagnets through a vacuum potential barrier was first probed by spin-polarized field emission spectroscopy (SPFES). Thus it has been reported that the low values of the polarization magnitude, below 10% for Ni, observed by SPFES [10–12] arise because the tunneling probability ratio between the  $4sp$  and the  $3d$  band lies in the range  $10^{-2} < T_d/T_{sp} < 10^{-1}$ , as predicted by theory [4–7].

In STM, however, the relative contribution of the  $3d$ -like states to the tunneling current appears to be greatly enhanced. This has been shown for the case of ferromagnetic tips on GaAs(110) [13] and possibly also explains the results of tunneling between a  $\text{CrO}_2$  tip and a Cr(001) surface [14]. The main difference between the STM and the SPFES geometry seems to reside in the thickness of the tunneling barrier, which is about a factor of 2 thinner in STM [15,16]. Thus the discrepancy between spin-polarized STM and SPFES results appears to be related to differences of the corresponding tunneling potential barrier parameters, e.g., their thickness and height.

To estimate quantitatively how the tunneling barrier height and thickness could influence the degree of the tunneling electron spin polarization, a simple model is used which assumes that the tunneling current arises from highly polarized  $3d$  and low polarized  $4sp$ -like contributions. Regarding the distinction between itinerant and localized  $3d$  states, we note that according to Ref. [8] the polarization of the  $d_l$  contribution is estimated to be +10%. In the SPSTM and SPFES measurements, however, the actual polarization is found to be of negative sign [10–12,16], except for Ni(110), which yields  $P = +(5 \pm 2)\%$  [12]. Additionally, as shown below, the SPSTM vs potential barrier thickness data provide no indication of a change of sign with potential barrier thickness as would be expected for competing localized vs delocalized  $3d$  states. For Fe, furthermore, the polarization of the  $d_l$  part is predicted to be 95% [8], whereas in SPFES it is reported to be at most +25% for emission

(tunneling) along [100] [17] and about +43% in SPSTM [16]. These observations favor an interpretation of vacuum tunneling where the  $4sp$ -like contributions are more important than the itinerant  $d_i$  part, at least when dealing with ferromagnetic tips. Thus for the analysis of the experimental data we assume that the tunneling current can be expressed as

$$i_T = i_d + i_{sp}, \quad (1)$$

where  $i_d$  and  $i_{sp}$  represent the contributions arising from the localized and the itinerant states, respectively. The tunneling current depends exponentially on the product of the tunneling barrier width and the square root of the mean barrier height,  $s_d\sqrt{\bar{\phi}_d}$  and  $s_{sp}\sqrt{\bar{\phi}_{sp}}$ , respectively. As the  $3d$  shells are more localized, we would expect  $s_d = s_{sp} + \delta s$ , where  $\delta s > 0$  is a small quantity relative to the typical values of  $s \approx 0.5$  nm. Thus one can make the approximation  $s_d = s_{sp} = s$ , and Eq. (1) can be written for small tunneling energies as

$$i_T = i_{d,0} \exp(-sA\sqrt{\bar{\phi}_d}) + i_{sp,0} \exp(-sA\sqrt{\bar{\phi}_{sp}}), \quad (2)$$

where  $i_{d,0}$  and  $i_{sp,0}$  are constants, and the decay length  $\kappa_j^{-1}$  for  $j = sp, d$  is related to the mean barrier height by  $\kappa_j = A\sqrt{\bar{\phi}_j}$ , where  $A = 2\sqrt{2m}/\hbar$ . Note that, because of image forces,  $\bar{\phi}_j$  is also a function of  $s$  [15,18,19]. The polarization  $P$  of the tunneling electrons is given by

$$i_T P = i_d P_d + i_{sp} P_{sp}, \quad (3)$$

where  $P_d$  and  $P_{sp}$  are the polarization of the  $3d$  and  $4sp$ -like states. From Eq. (2), assuming  $|P_{sp}| \ll |P_d|$  [5,7], it follows that

$$P(s) = \frac{P_d}{1 + (i_{sp,0}/i_{d,0}) \exp[sA(\sqrt{\bar{\phi}_d} - \sqrt{\bar{\phi}_{sp}})]}. \quad (4)$$

Note that the coefficient  $i_{j,0}$  is proportional to the local density of states near the Fermi energy multiplied by the nonexponential prefactor of the tunneling matrix element. The quotient of the pertinent prefactors is of the order of unity [20]. Thus one would expect  $i_{sp,0}/i_{d,0} \approx 3 \times 10^{-2}$ , which is approximately the ratio of the  $4sp$  to the  $3d$  band density of states at the Fermi level [21]. Because the relative tunneling probability is  $T_j \propto i_j$ , we obtain  $T_{sp}/T_d = i_{sp}/i_d$ , and thus Eq. (4) is equivalent to

$$P(s) = \frac{P_d}{1 + T_{sp}(s)/T_d(s)}. \quad (5)$$

Equation (4) shows that the decay length  $\kappa^{-1}$  of the tunneling electron spin polarization is a measure of the difference between the mean potential barrier heights,  $\kappa = A(\sqrt{\bar{\phi}_d} - \sqrt{\bar{\phi}_{sp}})$ . Because of their higher degree of spatial localization, the  $3d$ -like levels are expected to exhibit a shorter decay length at the surface than do the  $sp$ -like levels [22], implying that  $\bar{\phi}_{sp} < \bar{\phi}_d$ . From the above arguments we can see that, with decreasing barrier width, the tunneling probability for  $3d$ -like electrons should increase relative to the  $4sp$ -like states, thus giv-

ing rise to a relative increase of the highly polarized electron injection by tunneling across the barrier into the semiconductor.

The measurements of the electron spin polarization vs tunneling current were performed using ferromagnetic polycrystalline Ni tips and an  $\text{Al}_{0.06}\text{Ga}_{0.94}\text{As}(110)$  surface, which forms the tunneling barrier and acts as an optical spin detector. Typically, the tunneling current was varied in the range  $20 \leq i_T \leq 500$  pA, which causes the tip-surface distance to change by about 0.18 nm. The upper limit of the tunneling current was about 600 pA, at which point the tunnel junction usually becomes unstable, damage to the  $\text{Al}_{0.06}\text{Ga}_{0.94}\text{As}(110)$  begins to appear in the STM topographs, and the spin polarization degrades. The spin polarization of the tunneling electrons is determined by measuring the degree of circular polarization of the recombination luminescence. The luminescence induced by the tunneling current from the Ni tip into the  $\text{Al}_{0.06}\text{Ga}_{0.94}\text{As}(110)$  surface has a linear dependence on the tunneling current intensity. To check for background effects the recombination luminescence polarization was measured using nonmagnetic tips. There a small residual polarization can be detected, the magnitude of which decreases to zero near zero kinetic injection energy [13]; its magnitude is roughly an order of magnitude lower than the magnetic spin polarization effects reported here. Additionally, this residual effect has been further minimized by properly orienting the GaAs(110) surface such that the  $[\bar{1}, 1, 1]$  direction is perpendicular to the optical detection axis. Measurements of the spin polarization of electrons tunneling from ferromagnetic materials then reveal a negligible background, as can be seen in the raw data, Fig. 3 of Ref. [16]. For a detailed description of the technique and experimental details, see [13,16]. A typical  $P$  vs  $i_T$  result is shown in Fig. 1. The tunneling bias is  $V_T = 1.8$  V, which defines the probed binding energy range in the Ni tip,  $E_k \leq E < E_F$ , where  $E_k \approx eV_T - E_G = 300$  meV,  $E_G$  is the band gap of the semiconductor, and  $E_F$  is the Fermi energy. The data show that increasing the tunneling current from 20 to 500 pA gives rise to an increase of the spin polarization by about a factor of 2. Note that the relatively weak dependence of the spin polarization on the tunneling current indicates that its decay length is much longer than that for the tunneling current. To quantify this we note that Eq. (4) suggests the following relationship between the tunneling current and its spin polarization:

$$P = \frac{P_d}{1 + Bi_T^{-\gamma}}, \quad (6)$$

where  $P_d$ ,  $B$ , and  $\gamma$  are fitting parameters. As the total tunneling current can be expressed approximately by  $i_T = i_0 \exp(-sA\sqrt{\bar{\phi}})$ , where  $\bar{\phi}_{sp} < \bar{\phi} < \bar{\phi}_d$ , we see by comparison with Eq. (4) that  $\gamma$  is simply the ratio between the decay length of the tunneling current and the spin polarization:  $\gamma = (\sqrt{\bar{\phi}_d} - \sqrt{\bar{\phi}_{sp}})/\sqrt{\bar{\phi}}$ . The solid

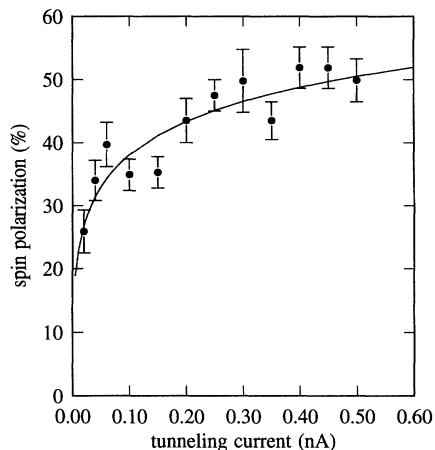


FIG. 1. Typical measurement of the tunneling electrons spin polarization as a function of the tunneling current. A ferromagnetic Ni tip is the source of spin-polarized electrons. An  $\text{Al}_{0.06}\text{Ga}_{0.94}\text{As}(110)$  surface forms the tunneling potential barrier and serves as an optical spin detector. The energy of the tunneling electrons lies in the range  $0 < E \leq 300$  meV. The variation of the tunneling current in the range  $20 < i_T < 500$  pA induces a change  $\Delta s \approx 0.18$  nm of the thickness of the potential barrier. The solid line is a fit of Eq. (6) to the data.

line in Fig. 1 is Eq. (6) fitted to the data. The result of several measurements yields  $\gamma = 0.35 \pm 0.06$ ; i.e., the spin polarization of the tunneling electrons has a decay length that is about 3 times longer than the decay length of the tunneling current. This result can be useful to estimate the relative magnitude of the barrier heights. Assuming  $\bar{\phi} = (\bar{\phi}_d + \bar{\phi}_{sp})/2$ , it is easy to show that  $\bar{\phi}_d - \bar{\phi}_{sp} \approx 2\gamma\bar{\phi}$ . An apparent barrier height of  $\bar{\phi}_d = 3.5$  eV was determined from  $d \ln i_T / ds$  measurements. To obtain the value of the actual mean barrier height, the reduction induced by the image forces has to be subtracted [15,18,19]. This reduction is approximately 1.5 eV for the tip-surface distances typical of these STM measurements [15]. Taking this correction into account one can estimate the barrier height difference to be  $2\gamma\bar{\phi} \approx 1.4$  eV. The assumption  $s_d = s_{sp} = s$  was made above. Because of the stronger localization of the  $3d$  levels, however, one would expect  $s_d < s_{sp}$ , which implies that the difference between the barrier heights estimated above is somewhat exaggerated. The fitting of Eq. (6) to the data indicates that the  $3d$ -like contributions are highly polarized and that the ratio  $i_{sp,0}/i_{d,0}$  varies by a factor of 2 or more between different measurements. For the particular results shown in Fig. 1 one can estimate  $0.42 \leq T_d/T_{ps} \leq 1.1$ , i.e., the probability ratio changes by a factor of 2.6 when the barrier width changes by  $\Delta s \approx 0.18$  nm. Note that this is an example that the  $3d$  contribution to the tunneling current can become dominant. In addition, the fit to the data in Fig. 1 yields the value  $i_{ps,0}/i_{d,0} = (4.0 \pm 2) \times 10^{-2}$  if we

set  $s = 0.50 \mp 0.05$  nm for  $i_T = 0.4$  nA. The actual magnitude of  $s$ , as far as it can be defined, lies within the range of values obtained from one-dimensional numerical calculations using the model developed by Koenraad and co-workers [23]. The above analysis was done neglecting the polarization of the itinerant states. Hybridization of the  $4sp$  levels [6] and the inclusion of  $d_i$ -like states [8] can give rise to a positive polarization of the itinerant contribution. An analysis of the data assuming  $P_{sp} > 0$  shows that the fitting parameter  $i_{sp,0}/i_{d,0}$  decreases with increasing magnitude  $P_{sp}$ , roughly by a factor of 2 when increasing  $P_{sp}$  from 0 to 25%, while the parameter  $\gamma$  is reduced very slightly. Therefore the present results also allow an interpretation that includes positively polarized itinerant contributions [6]. They cannot, however, be reconciled with an interpretation in which the tunneling current is dominantly of the  $d_i$ -like type.

Finally, one can estimate from Eq. (4) and the parameters determined from the STM data that for the spin polarization to decrease to the magnitude observed with FES,  $1\% \leq P \leq 10\%$ , it is necessary to increase the barrier width to  $0.9 \leq s \leq 1.3$  nm, which is precisely the thickness range of the tunneling barrier for typical FES working conditions [10–12]. Thus the present interpretation of the STM data can also account for the magnitude of the spin polarization measured on Ni tips with FES and shows that higher tunneling electron spin polarization may be achieved more generally with STM than with FES. Another important difference between the STM and FES results is the shape of the potential barrier [15]. Furthermore, the energy range of the tunneling electrons can be made much narrower under STM conditions. Thus the FWHM of the distribution of tunneling electrons is well below 300 meV for the present experiments, whereas in FES typically FWHM = 0.2–0.5 eV. This can be of importance in the case of Ni, because the highest polarization of the  $3d$  levels appears within a narrow energy range below the Fermi level.

The STM results presented here show that the polarization of electrons tunneling from Ni into a III-V semiconductor surface increases with a decreasing width of the tunneling barrier. This shows that the coupling between the  $3d$ -like states and the semiconductor increases faster than for the  $4sp$ -like states. Thus the electron spin polarization can be used as a tag that allows wave functions of different angular momentum to be distinguished in the tunneling experiment. A simple approximate relationship between the spin polarization and the tunneling current is derived, Eq. (6), which proves useful to determine the barrier height difference for tunneling from  $4sp$  and  $3d$  levels and yields plausible values for the ratio  $i_{sp,0}/i_{d,0}$ , which is approximately the ratio of the  $4sp$  to the  $3d$  density of states at the Fermi level.

It is a pleasure to thank U. Dürig for enlightening and fruitful conversations and H. W. M. Salemink for his valuable help in determining the tunneling barrier thickness

by means of numerical calculations. The  $\text{Al}_{0.06}\text{Ga}_{0.94}\text{As}$  was kindly provided by H. P. Meier. Many thanks also to R. Allenspach for many useful comments and a critical reading of the manuscript.

- 
- [1] *Magnetism and Structure in Systems of Reduced Dimension*, edited by R.F.C. Farrow, B. Dieny, M. Donath, A. Ferth, and B.D. Hermsmeier, NATO ASI, Ser. B, Vol. 309 (Plenum, New York, 1993).
- [2] Proceedings of the 5th NEC Symposium on Fundamental Approaches to New Material Phases. Spin Dependent Phenomena in Multi-Layer Systems, 16-20 October, 1994, Karuizawa, Japan [J. Mat. Sci. Eng. B (to be published)].
- [3] Proceedings of the International Workshop on Spin Polarized Electron Transport, 19-22 February 1995, Miami, FL [J. Magn. Magn. Mater. (to be published)].
- [4] J. W. Gadzuk, Phys. Rev. **182**, 416 (1969).
- [5] B. A. Polizer and P. H. Cutler, Phys. Rev. Lett. **28**, 1330 (1972).
- [6] J.-N. Chazalviel and Y. Yafet, Phys. Rev. B **15**, 1062 (1977).
- [7] A. Modinos, *Field, Thermionic and Secondary Electron Emission Spectroscopy* (Plenum Press, New York, 1984).
- [8] M. B. Stearns, J. Magn. Magn. Mater. **5**, 167 (1977); J. Appl. Phys. **72**, 5354 (1992).
- [9] R. Meservey and P. M. Tedrow, Phys. Rep. **238**, 173 (1994).
- [10] N. Müller, W. Eckstein, W. Heiland, and W. Zinn, Phys. Rev. Lett. **29**, 1654 (1972).
- [11] M. Landolt and M. Campagna, Phys. Rev. Lett. **38**, 663 (1977); Surf. Sci. **70**, 197 (1978).
- [12] M. Landolt, Y. Yafet, B. Wilkens, and M. Campagna, Solid State Commun. **25**, 1141 (1978).
- [13] S. F. Alvarado and Ph. Renaud, Phys. Rev. Lett. **68**, 1387 (1992).
- [14] R. Wiesendanger, H.-J. Güntherodt, G. Güntherodt, R. J. Gambino, and R. Ruf, Phys. Rev. Lett. **65**, 247 (1990).
- [15] S. F. Alvarado, in Ref. [3].
- [16] S. F. Alvarado, in *New Trends in Magnetism Magnetic Materials and Their Applications*, edited by J. L. Morán-López and J. M. Sanchez (Plenum, New York, London, 1994), p. 175.
- [17] M. Landolt and Y. Yafet, Phys. Rev. Lett. **40**, 1401 (1978).
- [18] G. Binnig, N. García, H. Rohrer, J. M. Soler, and F. Flores, Phys. Rev. B **30**, 4816 (1984).
- [19] J. G. Simmons, J. Appl. Phys. **35**, 2581 (1963).
- [20] C. J. Chen, *Introduction to Scanning Tunneling Microscopy* (Oxford University Press, New York, 1993).
- [21] D. A. Papaconstantopoulos, *Handbook of the Band Structure of Elemental Solids* (Plenum, New York, 1986).
- [22] M. Aldén, M. Mirbt, H. L. Skriver, N. M. Rosengaard, and B. Johansson, Phys. Rev. B **46**, 6303 (1992).
- [23] P. Koenraad, H. W. M. Salemink, and O. Albrektsen (to be published); H. W. M. Salemink, M. B. Johnson, U. Maier, P. Koenraad, and O. Albrektsen, in *Semiconductor Interfaces at the Sub-Nanometer Scale*, edited by H. W. M. Salemink and M. D. Pashley, NATO ASI, Ser. E, Vol. 243 (Kluwer, Dordrecht, 1993), p. 151.